Brain Structure and Function (2020) 225:1903–1919
https://doi.org/10.1007/s00429-020-02084-9

ORIGINAL ARTICLE

Association of γ-aminobutyric acid and glutamate/glutamine in the lateral prefrontal cortex with patterns of intrinsic functional connectivity in adults

Kai Wang[1,2] · Harry R. Smolker[2,3,4] · Mark S. Brown[5] · Hannah R. Snyder[6] · Benjamin L. Hankin[7] · Marie T. Banich[2,3]

Received: 12 October 2019 / Accepted: 4 May 2020 / Published online: 14 August 2020

Abstract

This study examined how levels of neurotransmitters in the lateral prefrontal cortex (LPFC), a region underlying higher-order cognition, are related to the brain's intrinsic functional organization. Using magnetic resonance spectroscopy (MRS), GABA+ and Glx (glutamate + glutamine) levels in the left dorsal (DLPFC) and left ventral (VLPFC) lateral prefrontal cortex were obtained in a sample of 64 female adults (mean age = 48.5). We measured intrinsic connectivity via resting-state fMRI in three ways: (a) via seed-based connectivity for each of the two spectroscopy voxels; (b) via the spatial configurations of 17 intrinsic networks defined by a well-known template; and (c) via examination of the temporal inter-relationships between these intrinsic networks. The results showed that different neurotransmitter indexes (Glx-specific, GABA+-specific, Glx-GABA+ average and Glx-GABA+ ratio) were associated with distinct patterns of intrinsic connectivity. Neurotransmitter levels in the left LPFC are mainly associated with connectivity of right hemisphere prefrontal (e.g., DLPFC) or striatal (e.g., putamen) regions, two areas of the brain connected to LPFC via large white matter tracts. While the directions of these associations were mixed, in most cases, higher Glx levels are related to reduced connectivity. Prefrontal neurotransmitter levels are also associated with the degree of connectivity between non-prefrontal regions. These results suggest robust relationships between the brain's intrinsic functional organization and local neurotransmitters in the LPFC which may be constrained by white matter neuroanatomy.

Keywords GABA+ · Glutamate · Lateral prefrontal · fMRI · MRS · Connectivity

Introduction

The goal of the present study was to examine how differences amongst individuals in the level of neurotransmitter in the lateral prefrontal cortex (LPFC) are associated with patterns of intrinsic functional connectivity across the brain. Glutamate (Glu) and gamma-Aminobutyric acid (GABA) are, respectively, the primary excitatory and inhibitory neurotransmitters in the brain. The majority of the total energy consumption in the brain is used to support glutamatergic

✉ Kai Wang
kaiwang@m.scnu.edu.cn

✉ Marie T. Banich
Marie.Banich@colorado.edu

[1] "Key Laboratory of Brain, Cognition and Education Sciences, Ministry of Education, China; School of Psychology, Center for Studies of Psychological Application, and Guangdong Key Laboratory of Mental Health and Cognitive Science, South China Normal University, No. 55 West Zhongshan Avenue, Guangzhou 510631, Guangdong, China

[2] Institute of Cognitive Science, University of Colorado Boulder, 344 UCB, Boulder, CO 80309-0344, USA

[3] Department of Psychology and Neuroscience, University of Colorado Boulder, E230 Muenzinger Hall, UCB 345, Boulder, CO 80309-0345, USA

[4] Institute for Behavioral Genetics, University of Colorado Boulder, 1480 30th Street, Boulder, CO 80303, USA

[5] Department of Radiology, University of Colorado Anschutz Medical Campus, 12401 E 17th Place, Aurora, CO 80045, USA

[6] Department of Psychology, Brandeis University, 415 South Street, Waltham, MA 02453, USA

[7] Psychology Department, University of Illinois-Urbana Champaign, 603 E. Daniel Street, Champaign, IL 61820, USA

neurotransmission (Magistretti et al. 1999; Attwell and Laughlin 2001), which is in turn modulated by GABAergic interneurons (Petroff 2002). As such, it is generally believed that macroscale neural activity is associated with regional levels of Glu, GABA or/and their ratio (Douglas and Martin 2004; Donahue et al. 2010).

In humans, the association between regional levels of these neurotransmitters and macroscale neuronal activity can be investigated via the combined use of two neuroimaging techniques. One, magnetic resonance spectroscopy (MRS), can provide proxy measures of the two neurotransmitters of interest, glutamate and GABA. Because of the relatively poor ability to separate distinct peaks in the spectra, MRS provides a measure of the sum of glutamate (Glu) and the associated and strongly correlated glutamine (Gln) which is often referred to as Glx (Glu + Gln). Similarly, it is difficult to isolate GABA specifically and hence the measure of GABAergic function derived from MRS is often referred to as GABA+, indicative of GABA and related peaks.

Another technique, functional magnetic resonance imaging (fMRI) allows a measure of macroscale neural activity as assessed by the BOLD signal (Logothetis et al. 2001; Buzsáki et al. 2007). The larger-scale functional organization of the brain can be determined from examining correlations of fMRI signals across the brain during rest, referred to as resting-state MRI (rs-fMRI; Fox and Raichle 2007; Deco et al. 2010). These connectivity patterns are relatively stable across multiple cognitive states (e.g., different task-states and resting-states; Fox and Raichle 2007; Smith et al. 2009; Cole et al. 2014) and likely reflect the intrinsic functional organization of the brain. Moreover, these patterns of connectivity tend to segregate into reproducible networks at various levels of granularity (e.g., Yeo et al. 2011). Importantly for the current study, longitudinal studies have shown that connectivity patterns are stable overtime for up to three years (Shehzad et al. 2009; Guo et al. 2012). Hence, intrinsic connectivity, measured at both voxel-wise and network-wise levels, is likely a good way to capture individual differences in the brain's intrinsic organization, as we do in the present study.

While the literature is relatively limited, at least some studies have combined these two techniques to determine how variations amongst individuals in regional levels of Glu and GABA are associated with patterns of brain organization and connectivity. Reviewing the existing literature across brain regions, Duncan et al. (2014) tentatively proposed that there is a trend for higher levels of GABA+ in a given brain region to be associated with reduced connectivity to other brain regions while higher glutamate levels in a region are associated with enhanced connectivity to distant brain regions. But the evidence is quite mixed. Consider one of the most commonly examined regions, the medial prefrontal cortex (mPFC), as an example. Some studies reported results that are in line with the trend proposed by Duncan et al. (2014) (Lianne et al. 2012; Shukla et al. 2019), while others reported results in the opposite direction (Horn et al. 2010; Delli Pizzi et al. 2017), and yet another study reported mixed results (Duncan et al. 2013).

Moreover, the prior work is not without limitations. One limitation is that, for the most part, studies have mainly focused on neurotransmitter levels in regions involved in lower-level sensory and motor processes (e.g., Stagg et al. 2014; Antonenko et al. 2017), social/emotional functions (e.g., Duncan et al. 2013), or regions that are more active during rest (e.g., Kapogiannis et al. 2013). In contrast, little is known about how individual differences in levels of these neurotransmitters in regions associated with higher-order cognitive function, such as lateral prefrontal cortex (LPFC), are associated with the brain's functional organization. Moreover, sample sizes in most prior studies were usually on the order of 20 or so individuals, which may be underpowered for correlational analysis (Yarkoni 2009). In the current study, we address both these issues by examining how intrinsic functional connectivity (as assessed by rs-fMRI) is related to individual differences in levels of GABA+ and glutamate (as assessed by MRS) in the lateral prefrontal cortex (LPFC), a region essential for executive functions, in a sample of 64 adults.

In our study, we measured neurotransmitter levels in two MRS voxels, one in a dorsal region (DLPFC) and the other in a ventral region of LPFC (VLPFC). Our motivation for doing so is that these two sub-regions are thought to support different aspects of executive function. DLPFC has been linked to maintaining task-relevant information and biasing current processing towards goal-related behavior, especially in the face of distraction (e.g., Miller and Cohen 2001; Banich 2009), whereas VLPFC is mainly involved in selecting amongst competing task-relevant information (Badre and Wagner 2007; Snyder et al. 2014), retrieving information from long-term memory (Badre and Wagner 2007), and language comprehension and production (Grodzinsky and Santi 2008; Fadiga et al. 2009). Moreover, studies of anatomical connectivity indicate that DLPFC sends information to and receives information from multimodal regions (e.g., parietal lobe and hippocampus), whereas VLPFC receives sensory inputs from multiple sources (for a review, see Tanji and Hoshi 2008). As such, we examined how individual differences in levels of GABA+ and Glx in two distinct voxels, one in DLPFC and another in VLPFC, are associated with patterns of intrinsic connectivity.

In our study, we examined a number of different measures of neurotransmitter function. Glutamate and GABA belong to a shared neurochemical pathway known as the GABA shunt, in which glutamine is the precursor of both glutamate and GABA (Reubi et al. 1978; Bak et al. 2006). To assess this common activity, one measure of interest was

the level of neurotransmitter in each voxel averaged across Glx and GABA+. However, we were also interested in the association of resting-state connectivity with each neurotransmitter specifically. To do so, we examined the relationship of connectivity with the level of each neurotransmitter, while co-varying out effects of the other, which we refer to as GABA+-specific and Glx-specific levels respectively. Finally, we also examined their ratio (Glx/GABA+) which is thought to reflect the relative balance of excitatory to inhibitory processing.

Based on the limited prior literature, we hypothesize that associations between neurotransmitter levels in LPFC and intrinsic connectivity patterns would be distinguishable from the associations observed previously involving neurotransmitters from other regions. Specifically, we predicted that: 1) individual differences in neurotransmitters in LPFC would be associated with intrinsic connectivity (see "Methods") of regions/networks both within and outside of the LPFC, due to the top-down and widespread influence of the LPFC, and 2) that GABA+-specific and Glx-specific levels, the ratio of Glx over GABA+, and the average level of GABA+ and Glx will have distinct influences on patterns of intrinsic connectivity.

Methods

Overview

This study tested how concentration levels of the major excitatory (Glx) and inhibitory (GABA+) neurotransmitters in DLPFC and VLPFC respectively, measured via magnetic resonance spectroscopy (MRS), are correlated with various aspects of intrinsic connectivity of the brain, measured via fMRI. For each MRS voxel, four measures of neurotransmitter levels were used (a) the average of Glx and GABA+, which reflects the common metabolic pathway of these two neurotransmitters, (b) the relative level of GABA+ controlling for Glx, to identify GABA+-specific contributions (c) the relative level of Glx controlling for GABA+, to identify Glx-specific contributions and (d) the ratio of Glx over GABA+ to examine the relative balance of excitatory to inhibitory neurotransmission. Three aspects of intrinsic connectivity were examined, including (1) seed-based connectivity using as seeds the MRS voxels in DLPFC and VLPFC from which the neurotransmitter signals were obtained, (2) the spatial configurations of 17 intrinsic connectivity networks, which were calculated for each individual based on a standard template (details below; Yeo et al. 2011), and (3) the temporal inter-relationships between these intrinsic connectivity networks. Results went through multiple types of stringent corrections for multiple comparisons (both voxel-wise and cluster-wise familywise error rate correction).

Participants

All participants were drawn from the greater Denver/Boulder metro area. They were all parents of youth in the Colorado Cognitive Neuroimaging Family Emotion Research (CoNiFER) study, who after an invitation to also participate in the study agreed to do so. Five fathers also agreed to participate in the study, but because their numbers were so low, only mothers ($N = 64$, mean age = 48.5, SD = 6.7 years) were included in the present analysis. All of the participants were drawn from separate families, with families drawn from an unselected community sample originally recruited to participate in the GEM (genes, environment and mood) study (NIH Grant R01 MH077195) and an associated follow-up study (R21MH102210). For details of the two samples and studies, see Hankin et al. (2015) and Snyder et al. (2019). These community samples were recruited from the Denver metro area, via public schools and using direct mail to target zip codes to maximize demographic and socioeconomic diversity. All participants were screened to be free of a history of neurological insult, spoke English as their first language, and did not report having dyslexia or difficulty reading. Informed consent was obtained from all participants and all procedures were approved by the University of Colorado Institutional Review Board.

Image acquisition and preprocessing

Image acquisition

A SIEMENS MAGNETOM PRISMA (3-T) MRI system with a 32-channel head coil was used for structural, functional, and MR spectroscopy data acquisition. To reduce head motion during MRI data acquisition, foam padding was placed around participants' heads. Data pertaining to gray matter structure was acquired via a T1-weighted Magnetization Prepared Gradient Echo sequence in 224 sagittal slices, with a repetition time (TR) = 2400 ms, echo time (TE) = 2.07 ms, flip angle = 8°, the field of view (FoV) = 256 mm, and a voxel size of 0.8 mm^3. Resting-state functional MRI data were acquired via gradient echo T2*-weighted echo-planar imaging (EPI). The axial acquisition geometry was as follows, TR = 460 ms, TE = 27.20 ms, flip angle = 44°, 56 slices, slice thickness = 3 mm, FoV = 248 mm, multi-band accel. factor = 8, gap = 1 mm, voxel size = 3.0 × 3.0 × 3.0 mm. A total of 640 frames (5 min) of resting-state data were acquired.

Following resting state acquisition, two MR spectroscopy voxels were placed following visible inspection of an individual subject's T1 structural image. The VLPFC voxel was positioned in the left inferior frontal gyrus anterior to the precentral gyrus and posterior to the frontopolar cortex (see Fig. 1 and white and yellow outlined regions in Fig. 3).

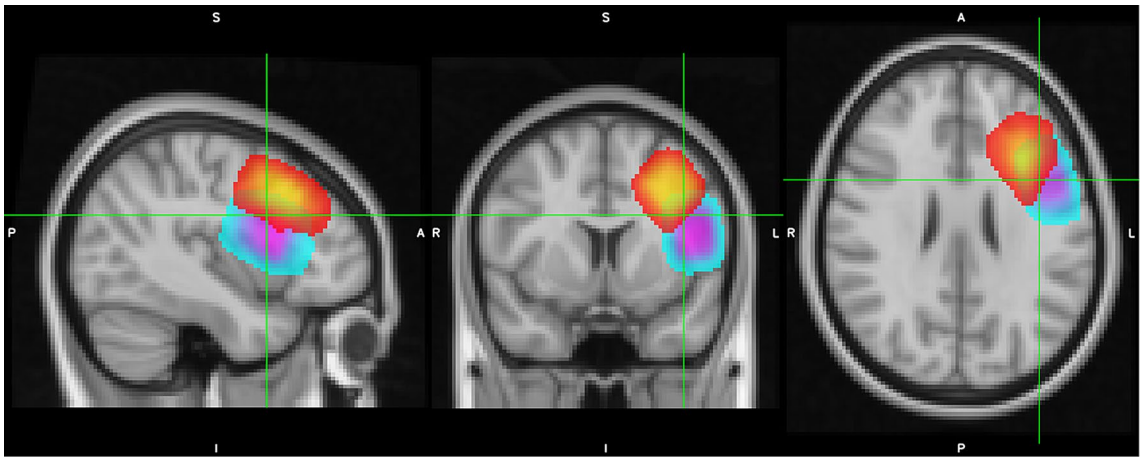

Fig. 1 Extent of coverage for MRS voxel placement for DLPFC (red–yellow) and VLPFC (blue–purple) voxels. Areas in red and cyan fell within the MRS voxel for 90% of all participants. Areas in yellow and purple fell within the MRS voxel for 75% of all participants

Care was taken to ensure that the voxel did not extend down into the insula or outside of brain tissue towards the skull. The DLPFC voxel was positioned in the left middle frontal gyrus (MFG), anterior to the precentral gyrus and posterior to the frontopolar cortex. Once again, care was taken to ensure that the voxel did not extend outside of brain tissue towards the skull. Mean voxel size across participants was 15.79 (2.00) mm^3 and 16.19 (2.48) mm^3 for the DLPFC and VLPFC voxels, respectively. The VLPFC voxel was larger than the DLPFC voxel because of the reduced area between the anterior and posterior landmarks in the middle as compared to inferior frontal gyrus.

Concentration levels of GABA+ and Glx were measured in each of these two voxels. Glx levels were measured using the PRESS sequence (TR/TE 2000/35 ms, 96 averages) and GABA+ was measured using the MEGA-PRESS sequence (Mescher et al. 1998) (TR/TE 2000/71 ms, 384 [192 edit-on, 192 edit-off] averages). Although Glx signals are obtained in the MEGA-PRESS spectrum, we chose to use Glx as determined from the PRESS data to avoid possible artifacts or baseline distortions on the Glx signal from the water suppression in the MEGA-PRESS sequence. Non-water suppressed spectra were acquired for both sequences in both voxels for water reference. Average water linewidth (FWHM) for both voxels was 10.0 Hz.

Image preprocessing

fMRI Processing and analysis of fMRI data were implemented using the FMRIB (Oxford Centre for Functional Magnetic Resonance Imaging of the Brain) Software Library package (FSL, version 5.0.8, www.fmrib.ox.ac.uk/fsl/). A first-level FEAT (FMRI Expert Analysis Tool) model was used for each individual for motion correction (MCFLIRT), high-pass filtering (200 s cutoff), spatial smoothing (FWHM = 5 mm), brain extraction (BET), non-linear registration to standard MNI152 and single-session independent component analysis (ICA) using MELODIC. Then FMRIB's ICA-based Xnoiseifier (FIX; version 1.062; Salimi-Khorshidi et al. 2014) was used to remove nuisance components from the data. We trained FIX based on this specific data set to optimize the effect of the tool (www.fsl.fmrib.ox.ac.uk/fsl/fslwiki/FIX). Components for data from 20 randomly selected subjects were hand-classified (by KW) into "good" and "bad" components. Sub-categories were specified for each bad component based on the features described in Salimi-Khorshidi et al. (2014). Classifiers were then trained based on these classifications and were applied (threshold: 20) to the remaining of subjects. Segmentation of individual's structure image into white matter and CSF was done with FSL's FAST tool (Zhang et al. 2001). Signals from white matter and CSF (FAST) were then regressed out (with command fsl_glm).

MR spectroscopy processing and analysis

The PRESS data were analyzed using the LCModel software (Provencher 1993) with an appropriate basis set from which the GLX values were obtained, while the MEGA-PRESS data were analyzed for using the Gannet MATLAB scripts (Edden et al. 2014) and employing the water signal from the non-suppressed spectra for intensity reference. CSF, grey matter, and white matter of the voxels were segmented via calls from Gannet to SPM12 (Functional Imaging Laboratory [FIL], The Wellcome Trust Centre for NeuroImaging, in the Institute of Neurology at University College London, UK). No correction for co-edited macromolecules was done either at acquisition or in processing and as such the GABA results are denoted as GABA+. All concentration levels are given as institutional units (i.u.; Fig. 2). Concentration levels

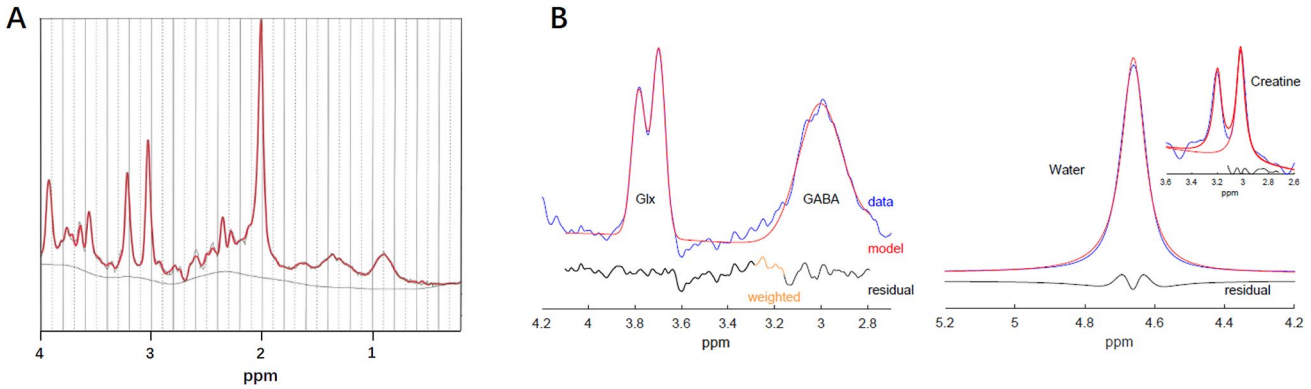

Fig. 2 Representative MRS spectra Signal from one participant, with water as reference. **a** PRESS Spectrum, used for Glx. **b** MEGA-PRESS spectrum used for GABA+ (shown to the right are fits for water and creatine references). These examples are from the dorsal voxel; the data from the ventral voxels were not distinguishable from the dorsal voxels by eye. *X* axis represents parts per million (ppm). No *y* axis is shown as the intensity of these signals are in institutional units

were adjusted for the proportion of gray matter within each voxel by dividing raw spectroscopy values by the proportion grey matter within each the DLPFC and VLPFC voxels, respectively. While some researchers control for the proportion of gray matter plus 0.5 times the proportion of white matter (Harris et al. 2015), values using this method were highly correlated (most greater than 0.9) and as such just the proportion of gray matter was used.

All MRS data points were reviewed by an expert in MRS acquisition and analyses who was not involved in carrying out the resting state analyses (author MSB). Spectroscopy data points were excluded if the MRS spectra (1) did not have discernable peaks coinciding with the neurotransmitters of interest or (2) was saturated with a signal indicative of considerable fat within the voxel of interest, suggesting voxel placement was suboptimal or (3) if the spectra showed artifacts suggestive of motion or other causes. This process results in adequate data for 62 participants for the VLPFC voxel and a subset of 57 participants for the DLPFC voxel.

Lower-level fMRI analyses

Seed-based analyses

We set the DLPFC and VLPFC voxels from which the MRS signals were acquired as seed regions. Because the exact extent of the voxels varied by the participant, we used as a seed the location that yielded the highest level of overlap for the largest number of participants. The dorsal voxel was centered at $x = -32$, $y = 18$, $z = 34$ (MNI coordinates) which fell within the dorsal voxel for 96% of all our participants, while the ventral voxel was centered at $x = -44$, $y = 12$, $z = 16$, which fell within the ventral voxel for 98.6% of our participants. Each seed region was a sphere of width 18 mm in diameter to reflect the large size of the voxel from which our data were drawn.

The seed regions were then registered back to participants' native space with FSL command "applywrap". Then average time series were extracted from the seed regions with FSL command "fslmeants". The time series were then put into a lower-level FEAT model where preprocessing options were turned off since the data were already pre-processed. This yielded per-voxel effect size parameter estimate (β) maps representing the correlation between each voxel and each seed region used in group-level statistical analyses. Voxel-wise whole-brain connectivity of the seed regions was obtained for each participant. Then the degree to which neurotransmitter levels in DLPFC and separately in VLPFC are related to seed-based connectivity were examined at the group level.

Network-based analyses

To define functional networks within the brain, we used a template from a study involving approximately 1000 participants, which has shown that activity of the human cerebral cortex at rest can be reliably organized into 17 intrinsic connectivity networks (Yeo et al. 2011). Here, we tested how concentrations of GABA+ and Glx are related to features of the 17 networks, including spatial configurations of these networks and the dynamic temporal relationships between these networks. See Fig. 3 for our labelling of these networks.

Analysis of network spatial composition We generated subject-specific versions of these 17 networks, including the spatial maps and associated time series data, using dual regression (Nickerson et al. 2017). First, for each subject, each of the spatial maps of the 17 networks is regressed (as

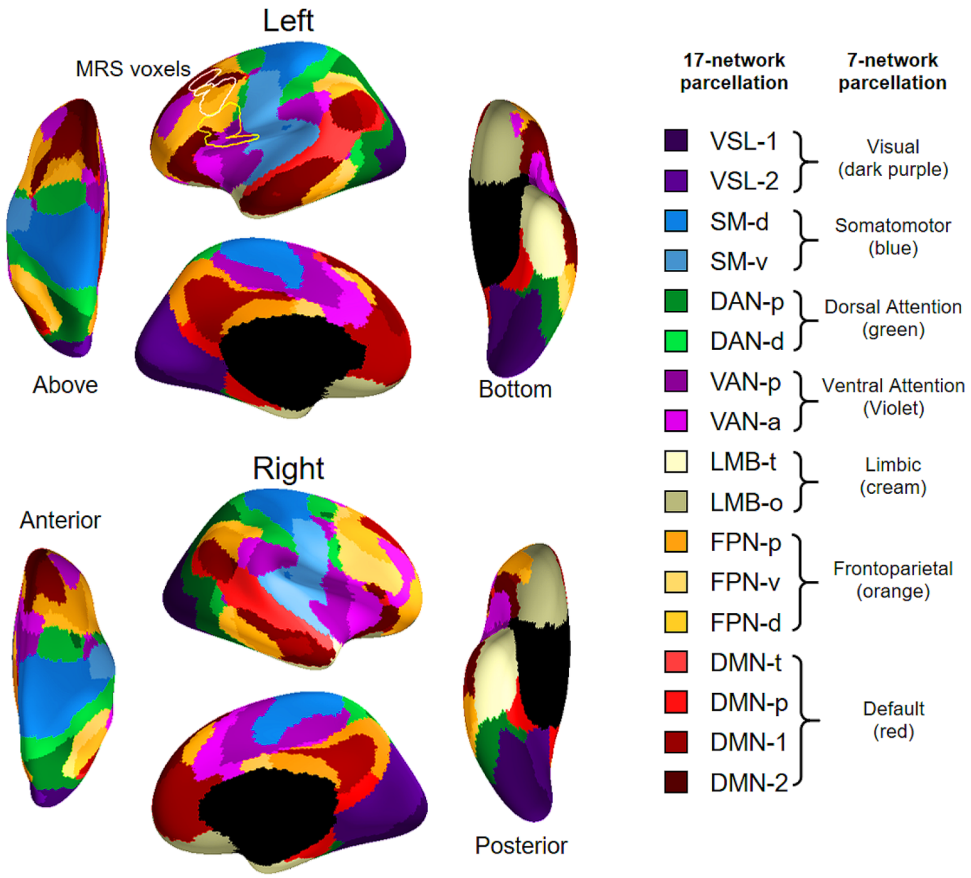

Fig. 3 Labels for the 17-network parcellation used in the network-based analyses. Locations of the two MRS voxels are outlined on the surface (white outline, DLPFC; yellow outline, VLPFC). These 17 networks are essentially sub-networks of a lower-resolution 7-network parcellation whose labels were offered in the original paper (Yeo et al. 2011). Due to the lack of labels for the 17-network parcellation in the original paper, we have labelled them as subnetworks of the 7-network parcellation. There are two visual subnetworks (shown in shades of purple) in the occipital region area (VSL-1 and VSL-2). The somatomotor network (shown in shades of blue) is divided into a dorsal somatomotor subnetwork (SM-d) and a ventral subnetwork (SM-v). The dorsal attention network (shown in shades of green) is divided into more anterior (DAN-a), and posterior parts (DAN-p). The ventral attention network (shown in shades of violet) likewise is divided into a more anterior (VAN-a) and posterior (VAN-p) portion. The limbic network (shown in cream/grey) is divided into a temporal portion (LMB-t) and an orbitofrontal portion (LMB-o). The frontoparietal network (shown in shades of orange) is divided into a posterior portion (FPN-p), a dorsolateral portion (FPN-d) and a ventrolateral portion (FPN-v). Finally, the default network (shown in shades of red/brown) contains a temporal portion (DMN-t), a posterior portion (DMN-p) and two smaller subnetworks (DMN-1, DMN-2)

spatial regressors in a multiple regression) into the subject's 4D space–time fMRI data. This results in a set of subject-specific time series, one for each of the 17 networks. Next, those time series are regressed (as temporal regressors, again in a multiple regression) into the same 4D dataset, resulting in a set of subject-specific spatial maps (resolution, 2 $mm^3 \times 2$ $mm^3 \times 2$ mm^3), one for each of the 17 networks. The spatial component maps were used in group-level statistical analyses. Our neurotransmitter measures were then used to examine how individual differences in these measures is associated with the spatial composition of the 17 networks.

Analysis of temporal correlations between networks To measure the temporal relationship between the 17 networks for each individual, time series of these networks, as generated by dual regression were fed into the FSLNets toolbox (v0.6; https://fsl.fmrib.ox.ac.uk/fsl/fslwiki/FSLNets). A 17 by 17 network matrix (or connectome) was created for each participant, with each matrix element representing the correlation strength between a given pair of networks. Both full correlation matrices (Pearson correlation) and partial correlations matrices, which partial out influences from any other element in the matrix, were calculated. Matrix values were converted from Pearson correlation scores (r values) into z statistics with Fisher's transformation.

To display the hierarchical nature of network connectivity, the group averaged full correlations were used as they are more powerful to identify such low-dimensional clustering patterns (Fig. 4; Smith et al. 2015). Hierarchical clustering

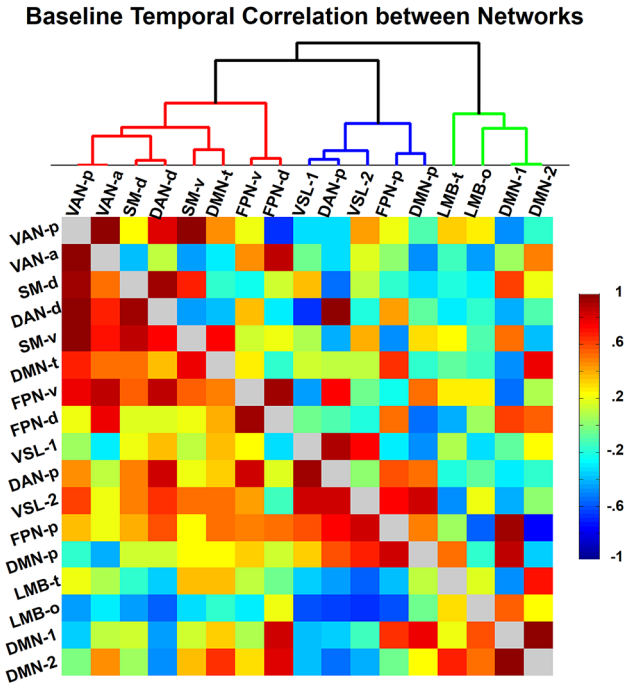

Fig. 4 Temporal signal correlation between 17 intrinsic networks averaged across participants. The dendrogram at the top shows a hierarchical clustering pattern based on full connectivity between networks. Three larger clusters are revealed, **a** motor-executive cluster shown in red, **b** visual-attention networks in blue and **c** default-limbic cluster in green. Plotted below diagonal are Pearson correlations which drive the cluster pattern. Plotted above the diagonal are partial correlations (controlling for other relationships in the matrix), which were used later in analyses with neurotransmitter variables as covariates. Correlations were converted to *Z* values via a Fisher's transformation

was carried out using Ward's method implemented in Matlab (see branch structure above the correlation matrix in Fig. 4). The pattern observed for our sample was in line with what has been observed for larger samples.

We then used the partial correlation in network connectivity to test the neurotransmitters' influence on network connectivity in group-level analyses, because it reflects direct connection strengths between networks (Marrelec et al. 2006). To improve the stability of the estimates of partial correlation coefficients, a small amount of L2 regularization is applied (setting rho = 0.01 in the Ridge Regression netmats option in FSLNets).

Group-level analyses and statistics

To test how neurotransmitter concentrations in LPFC are related to resting-state connectivity profiles, permutation tests were performed for statistical inference at the group level using the FSL's tool of Permutation Analysis of Linear Models (PALM; Winkler et al. 2014). PALM allows modelling and inference using standard GLM design setup files that were generated via FSL command "Glm". Three models were run for each MRS voxel. The first model has the average level of GABA+ and Glx as the explanatory variable (EV) or regressor of interest, and a group average (a vector of 1 s) and age as control EVs. The second model included four EVs including the level of Glx, level of GABA+ , age and group average. As a result, the effect of a neurotransmitter from this model controls for the impact of the other neurotransmitter in the same MRS voxel as well as age. Significant effects from this model will be referred to as Glx-specific and GABA+ -specific as they represent the unique contribution of each of these neurotransmitters after taking covariation with the level of the other neurotransmitter into account. The third model contains EVs of the ratio of Glx over GABA+ as the EV of interest and the group average and age as additional EVs. For all analyses, 10,000 permutations were performed for each contrast. The effects of the covariate neurotransmitter variables were tested via permutation with sign-flipping (supplying the "-ise" option).

Neuroimaging studies typically adopt voxel-wise or cluster-wise corrections for multiple comparisons in statistical inference. Compared to cluster-wise methods, voxel-wise methods allow for finer spatial specificity (Nichols 2012) and better control over false discoveries (Eklund et al. 2016). However, one disadvantage of voxel-wise methods is its lower sensitivity or higher likelihood in committing a Type II error (Lieberman and Cunningham 2009), compared to cluster-wise methods (Nichols 2012; Woo et al. 2014). Given that advantages of the two methods are complementary, we reported results with both voxel-wise and cluster-wise methods. After permutation, results were corrected for familywise error rate (FWER; Winkler et al. 2014) with $p < 0.05$. For cluster-wise correction, the cluster-forming threshold was $p < 0.001$. Then values of cluster mass (sum of t values within the cluster) were used as they are more sensitive than cluster size (Bullmore et al. 1999; Hayasaka and Nichols 2003). For the analysis of inter-network temporal correlations where cluster-wise inference does not apply, a threshold of $p < 0.005$ was also considered in addition to the more stringent familywise error rate correction.

Results

Spectroscopy measures

Mean and standard deviations

The levels of neurotransmitter for each neurotransmitter and each voxel are shown in Table 1.

Table 1 Descriptive statistics of neurotransmitters and correlation between neurotransmitter and age

	Dorsal Glx	Dorsal GABA+	Ventral Glx	Ventral GABA+
Mean	21.95	2.18	19.14	1.84
SD	4.89	0.67	3.29	0.40
Correlation with age	−0.13	−0.33**	0.28*	−0.24#

Neurotransmitter intensity is in institutional units

#$p < 0.075$, *$p < 0.05$, **$p < 0.01$

Table 2 Correlation between levels of Glx and GABA+

	Dorsal_Glx	Dorsal GABA+	Ventral Glx
Dorsal Glx			
Dorsal GABA+	0.71***/*0.71***		
Ventral Glx	0.33*/*0.37***	0.15/*0.25* #	
Ventral GABA + +	0.25#/*0.22*	0.35**/*0.27**	0.07/*0.17*

Base correlation shown in regular font, age-adjusted in italic

***$p < 0.0001$, **$p < 0.01$, *$p < 0.05$, #$p < 0.075$

Analysis of spectroscopy levels as a function of age

Given the limited prior research, we wished to examine the correlation between levels of neurotransmitters in our two LPFC voxels and age. As shown in Table 1, there were significant or marginally significant effects suggesting that generally (but not always) that there are decreasing levels of neurotransmitter with increasing age. As such, all subsequent analyses controlled for age.

Analysis of individual differences in levels of neurotransmitter across the two PFC voxels

Due to limited prior research, we also explored the correlation between neurotransmitter levels in each of the two PFC voxels, dorsal and ventral, for the 57 participants for whom we had a full data set. The results are shown in Table 2 (base correlation shown in regular font, age-adjusted in italics). They suggest that Glx and GABA+ levels are more correlated for the dorsal than the ventral voxel. Hence, in the neuroimaging GLM models we examined the specific influence of a given neurotransmitter (e.g., Glx) taking into account the level of the other neurotransmitter (e.g., GABA+) from the same voxel (e.g., DLPFC voxel).

Relationship between spectroscopy and intrinsic connectivity

Seed-based analyses

The goal of the seed-based analysis was to examine the connectivity of the regions from which the of neurotransmitter levels were obtained, with DLPFC and VLPFC used separately as seed regions. The average level of Glx and GABA+ in the VLPFC voxel was positively related to the connectivity between the DLPFC seed region (which was in the left hemisphere) and a portion of the right middle temporal gyrus which is part of the FPN-d network (Table 3 and Fig. 5A1). In addition, VLPFC Glx-specific levels were negatively related to the connectivity between the DLPFC seed region and right MFG (Table 3 and Fig. 5A2). The baseline seed-based connectivity for both effects was weakly positive (Fig. 5B).

Network-based analyses: spatial composition

As expected, voxel-wise FWER corrected results (Table 4) were more conservative than cluster-wise FWER corrected results (Table 5). Nevertheless, four effects survived both types of corrections (see Fig. 6 and bolded rows in Tables 4 and 5). First, there was a negative correlation between an individual's ventral Glx-specific level and the connectivity between SM-d and right MFG (Fig. 6A). Second, there was a negative correlation between the ratio of Glx over GABA+ in DLPFC and the connectivity between FPN-v network and right middle frontal gyrus (MFG; Fig. 6B). Third, a positive correlation was found

Table 3 Association between average neurotransmitter levels and seed-based intrinsic connectivity

Neurotrans-mitter	Seed	Direction	Label	Net	Size	BA	*T*	*X*	*Y*	*Z*
C-FWE										
V_Glx-specific	DLPFC	–	Right middle frontal gyrus	VAN-a	272	46	4.29	32	48	24
V-FWE										
V_AVG	DLPFC	+	Right middle temporal gyrus	FPN-d	2	20	5.25	62	−24	−22

AVG the average neurotransmitter level across Glx and GABA+, *"+"* higher neurotransmitter levels are related to increased connectivity strength. *"–"* Higher neurotransmitter levels are related to reduced connectivity strength. *Label* the anatomical name of the effect location, *Net* name of network the effect region locates in, BA Broadman Area, *"T" t* statistic value. *"X", "Y" and "Z"* MNI coordinate of the effect, *V-FWE* result passed voxel-wise FWER correction, *C-FWE* result passed cluster-wise FWER correction

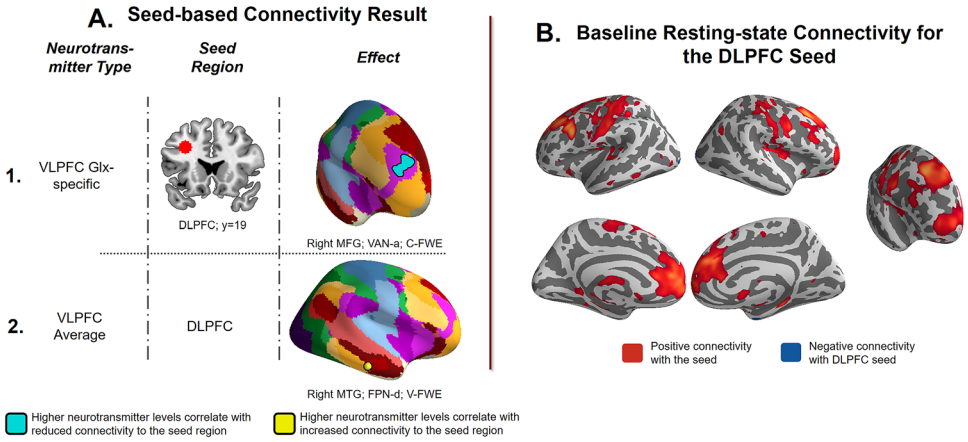

Fig. 5 **A** Correlation between individual differences in LPFC neurotransmitter concentrations and seed-based connectivity, with cluster-wise FWER correction. **B** Average resting-state connectivity of the DLPFC seed across all participants. Plotted is the *t* map thresholded at $t > 1.645$ ($p = 0.05$, one tail). V-FWE = result passed voxel-wise FWER correction. C-FWE = result passed cluster-wise FWER correction

Table 4 Covariate effect of neurotransmitters on spatial compositions of intrinsic networks with voxel-wise FWER correction

Neurotrans-mitter	Network	Direction	Label	Net	Size	BA	*T*	*X*	*Y*	*Z*
D_Glx-specific	DNN-t	+	Right anterior cingulate cortex	DMN-1	6	11	6.54	4	32	-4
V_Glx-specific	**SM-d**	**–**	**Right middle frontal gyrus**	**DMN-1**	**2**	**9**	**5.62**	**24**	**32**	**38**
D_GABA+-specific	DNN-t	–	Right anterior cingulate cortex	DMN-1	1	11	5.95	4	32	-4
D_Glx/GABA+	**FPN-p**	**+**	**Right putamen**		**3**		**5.71**	**20**	**4**	**−8**
D_Glx/GABA+	**FPN-v**	**–**	**Right middle frontal gyrus**	**FPN-d**	**2**	**45**	**5.43**	**44**	**30**	**40**
V_Glx/GABA+	DMN-p	+	Right lingual gyrus	VSL-2	2	19	5.84	18	−48	0
D_AVG	DAN-p	–	Right putamen		1		5.32	30	−10	−28
D_AVG	FPN-p	+	Right gyrus rectus	LMB-o	1	11	5.57	8	34	−22
V_AVG	FPN-d	+	Left orbital frontal cortex	FPN-d	4	47	5.86	−34	58	−10
V_AVG	SM-d	–	Left superior frontal gyrus	DMN-1	2	32	6.26	−18	32	40
V_AVG	**DMN-1**	**+**	**Right middle frontal gyrus**	**VAN-a DMN-1**	**1**	**9**	**6.23**	**30**	**36**	**34**

Effects passed both voxel-wise and cluster-wise FWER corrections are shown in bold and plotted in Fig. 6. "D" and "V" in the first column indicate the DLPFC and VLPFC MRS voxels respectively

AVG averaged level of Glx and GABA+ in that MRS voxel, *Glx/GABA+* the ratio of Glx over GABA+, *"+"* higher neurotransmitter levels are related to expanded network extent or increased connectivity strength, *"–"* higher neurotransmitter levels are related to reduced network extent or decreased connectivity strength, *"Label"* the anatomical name of the effect location, *Net* name of network the effect region locates in, *BA* Broadman Area, *"Size"* cluster size of the effect, *"T" t* statistic value, *"X", "Y" and "Z"* the MNI coordinate of the effect

between the ratio of Glx over GABA+ in DLPFC and the connectivity between the FPN-p network and right putamen (Fig. 6B). Fourth, the greater a participant's with higher overall neurotransmitter levels (averaged across GABA + and Glx), the more their SM-d network was less connected to a region in middle frontal gyrus that resides in VAN-a and DMN-1 (Fig. 6A).

Network-based analyses: temporal correlations

No effect passed the stringent FWER correction. We report in Table 6 effects that passed the threshold of $p < 0.005$. Notably, the temporal relationship between subnetworks of DMN and LMB-o were related to various metrics of neurotransmitter levels for both the dorsal and ventral voxels.

Discussion

With a decent sample size, the present study demonstrated robust relationships between individual differences in concentration levels of GABA + and Glx in DLPFC and VLPFC with patterns of intrinsic connectivity of the brain. Neurotransmitter levels were found to be related to multiple aspects of intrinsic connectivity, including seed-based connectivity profiles (with DLPFC and VLPFC being the seed regions), spatial composition, and the temporal relationships of activity between networks. To our knowledge, this is the first report of such relationships.

Table 5 Covariate effect of neurotransmitters on spatial compositions of intrinsic networks with cluster-wise FWER correction

Neurotrans-mitter	Network	Direction	Label	Net	Size	BA	*T*	*X*	*Y*	*Z*
D_GABA+-speicifc	VSL-2	–	Right putamen		441		5.14	20	4	−8
			Right amygdala				4.66	26	−4	−14
			Right anterior insula	VAN-p			4.54	36	14	6
			Right caudate nucleus				4.14	16	10	10
D_GABA+-specific	FPN-p	–	Right putamen		239		4.94	28	2	−8
			Right amygdala				4.9	26	−4	−16
V_Glx-specific	**SM-d**	**–**	**Right middle frontal gyrus**	**DMN-1**	**389**	**9**	**5.62**	**24**	**32**	**38**
			Right superior frontal gyrus	DMN-1		9	4.72	24	42	46
			Left middle frontal gyrus	VAN-a	207	46	4.68	−28	36	26
			Left inferior frontal gyrus	FPN-v		45	4.66	−44	24	28
			Left superior frontal gyrus	DMN-1	141	32	5.35	−16	32	42
			Left anterior cingulate cortex	VAN-a		32	3.44	−14	32	28
V_GABA+-specific	SM-v	–	Left middle temporal gyrus	DMN-2	661	37	5.56	−58	−54	38
			Left supramarginal gyrus	FPN-d		39	5.01	−48	−46	34
				DMN-2						
			Left inferior parietal lobule	FPN-v		40	5.01	−48	−46	48
				FPN-d						
			Left angular gyrus	DMN-1		39	4.84	−46	−64	44
			Left superior parietal lobule	DAN-p		7	4.69	−26	−62	56
			Left angular gyrus	DMN-2		39	3.98	−58	−60	26
			Left inferior parietal lobule	DAN-p		40	3.88	−38	−58	58
				FPN-d						
V_GABA+-specific	VAN-p	+	Right middle occipital gyrus	DAN-p	463	39	5.4	40	−76	22
			Right inferior occipital gyrus	VSL-1		19	5.38	38	−86	−10
			Right superior occipital gyrus	VSL-1		19	5.18	26	−78	26
			Right fusiform gyrus	VSL-1		19	4.43	32	−78	−2
			Right lingual gyrus	VSL-1		18	4.11	24	−90	−6
			Right calcarine cortex	VSL-2		19	3.65	16	−84	14
V_GABA+-specific	LMB-t	+	Left temporal pole	LMB-t	4294	38	5.7	−40	20	−32
			Left insular cortex	VAN-p			5.6	−36	6	4
			Left temporal pole	LMB-t		36	5.53	−30	14	−36
			Left fusiform gyrus	LMB-t		36	5.43	−36	−4	−30
			Left caudate nucleus				5.42	−8	8	16
			Left inferior temporal gyrus	LMB-t		36	5.24	−36	−2	−42
			Left hippocampus				5.08	−26	−6	−16
			Left temporal pole	DMN-2		38	5.04	−50	12	−32
			Right caudate nucleus				4.81	12	−2	20
			Left temporal pole	SM-v		38	4.75	−52	10	−10
			Left fusiform gyrus	LMB-t		20	4.67	−38	−24	−24
			Left parahippocampal gyrus	LMB-t			4.57	−24	0	−32
			Left inferior temporal gyrus	LBM-t		20	4.54	−46	−16	−28
			Left inferior temporal gyrus	DMN-2		20	4.51	−50	−6	−36
				LMB-t						
			Left middle temporal gyrus	DMN-2		21	4.48	−62	−8	−22
			Right thalamus				4.27	6	−16	18
			Left putamen				4.21	−18	8	8
			Left insular cortex	VAN-p			4.13	−38	−2	−6
			Left putamen				4.1	−28	4	14
			Left fusiform gyrus	LBM-t		20	3.93	−24	−4	−44

Table 5 (continued)

Neurotrans-mitter	Network	Direction	Label	Net	Size	BA	*T*	*X*	*Y*	*Z*
V_GABA+-specific	DMN-p	+	Left middle temporal gyrus	DMN-2	1205	20	5.87	−46	−18	−12
			Left fusiform gyrus	DAN-p		37	5.58	−38	−38	−22
			Left inferior temporal gyrus	FPN-v		20	4.93	−54	−42	−24
			Left middle temporal gyrus	DMN-2		22	4.34	−66	−16	−6
			Left middle temporal gyrus	DMN-2		22	4.08	−58	−8	−10
D_Glx/GABA+	**FPN-p**	**+**	**Right putamen**		**127**		**5.71**	**20**	**4**	**−8**
			Right putamen				3.8	24	−4	−16
D_Glx/GABA+	**FPN-v**	**–**	**Right middle frontal gyrus**	**FPN-d**	**122**	**45**	**5.43**	**44**	**30**	**40**
			Right middle frontal gyrus	FPN-d		46	3.81	34	20	38
V_AVG	**SM-d**	**–**	**Right middle frontal gyrus**	**VAN-a**	**448**	**9**	**6.23**	**30**	**36**	**34**
			Right superior frontal gyrus	DMN-1		9	5.83	18	40	42
V_AVG	VAN-a	+	Right middle frontal gyrus	VAN-a	474	46	5.42	26	56	26
			Right middle frontal gyrus	VAN-a		46	4.99	38	50	22
			Right middle frontal gyrus	VAN-a		9	4.72	32	42	38

Effects passed both voxel-wise and cluster-wise FWER corrections are shown in bold and are plotted in Fig. 7. An effect may involve more than one cluster, for which all local peaks were reported (minimal distance = 12 mm). Clusters lacking a "Size" value are those involving local peaks within the cluster noted above

AVG averaged level of Glx and GABA + + in that MRS voxel, *"D" and "V"* in the first column indicate the DLPFC and VLPFC MRS voxels respectively. *Glx/GABA+* the ratio of Glx over GABA+, *"+"* higher neurotransmitter levels are related to expanded network extent or increased connectivity strength, *"–"* higher neurotransmitter levels are related to reduced network extent or decreased connectivity strength. *Label* the anatomical name of the effect location, *Net* name of network the effect region locates in, *BA* Broadman Area, *"T" t* statistic value, *"X", "Y" and "Z"* the MNI coordinate of the effect

Major findings

Overall, the results can be classified into two categories. First, individual differences in the level of LPFC neurotransmitters are associated with intrinsic connectivity of an LPFC region or a network significantly involving the LPFC. Second, LPFC neurotransmitters are associated with connectivity patterns of regions or networks outside the LPFC. Therefore, as we predicted, LPFC neurotransmitter's relevance to intrinsic connectivity seems not to be limited to the LPFC. Below we discuss these two groups of results separately.

Left LPFC neurotransmitter levels are associated with connectivity of LPFC regions or networks significantly involving the LPFC

Both the seed-based connectivity analysis and the spatial composition analysis indicated that LPFC neurotransmitter levels, which we assessed in the left prefrontal cortex, are associated with the characteristics of connectivity in regions of the right prefrontal cortex. In the seed-based analyses, connectivity of the left DLPFC seed and a region in the right MTG was influenced by individual differences in levels of the neurotransmitter in the left VLPFC (Fig. 5A). In the spatial composition analysis, the connectivity of portions of the right DLPFC (to the SM-d and FPN-v respectively) were related to neurotransmitter levels in the left LPFC (see a, c and d in Fig. 6). To understand the nature of these associations, one may consider facts in anatomy and physiology that underlie bilateral LPFC communication.

The corpus callosum (CC) is the major connective pathway between the two hemispheres. Recent evidence, primarily from lesion studies, suggested that CC is even more essential in interhemispheric communications between higher-level associative regions, like the LPFC than in communications between lower-level brain regions, e.g., the primary visual areas (Fame et al. 2011; Roland et al. 2017). The great majority of callosal projection neurons are glutamatergic pyramidal neurons (Jacobson and Trojanowski 1974; Conti and Manzoni 1994), yet a small portion of them are GABAergic (Rock et al. 2017). Thus, the transmission of glutamate (or potentially GABA) is essential for any neuronal communication between LPFC regions via the CC. Moreover, in the prefrontal cortex, callosal neurons synapse not only on glutamatergic pyramidal neurons but also on GABA interneurons (Carr and Sesack 1998; Iacoboni and Zaidel 2003). Therefore, one would expect neurotransmitter levels of LPFC in one hemisphere could influence functioning in the other hemisphere, as is reflected in the well-powered interhemispheric associations observed in the current study.

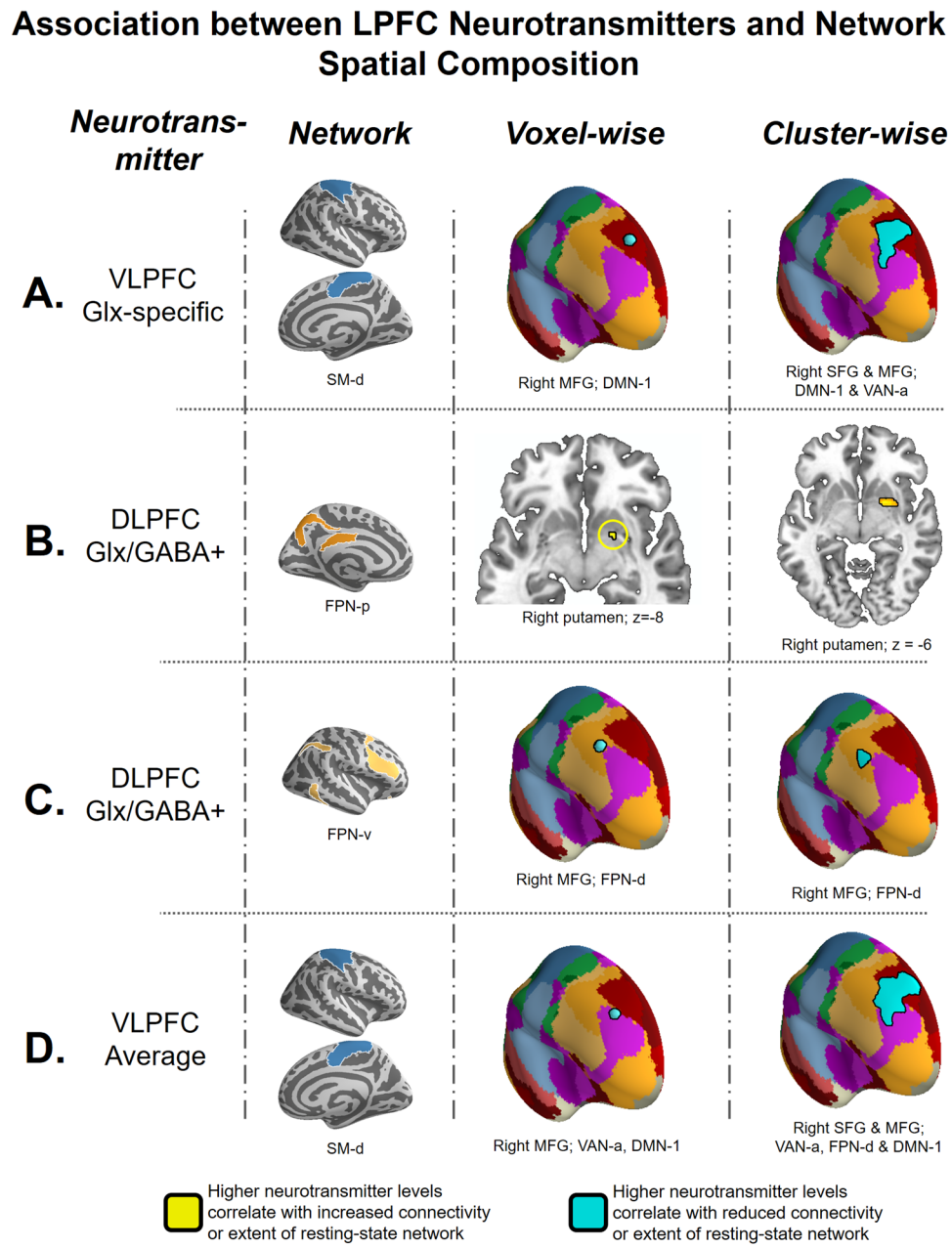

Fig. 6 Correlations between neurotransmitters in LPFC and spatial compositions of intrinsic networks. These results passed both voxel-wise and cluster-wise FWER corrections (shaded rows in Tables 4 and 5). Each effect involves the neurotransmitter involved (first column), the network being affected (second column), and an effect location (third column with voxel-wise FWER correction and fourth column with FWER cluster-wise correction; the caption below noted the anatomical label and the intrinsic network the effect falls in). Since clusters are small for voxel-wise corrected effects, a sphere of 1 cm diameter is plotted at the peak location of each effect. *MFG* middle frontal gyrus. *Glx/GABA+* the ratio of Glx over GABA+

Many of our findings are consistent with the structure of certain major interhemispheric white-matter pathways of the prefrontal cortex. Recently, combining post-mortem microdissection and advanced diffusion tractography imaging which better detects lateral fiber tracts, De Benedictis et al. (2016) examined the structural macroscopic connectivity of the frontal fibers of the CC. One of the three major pathways they found, the ventro-lateral pathway, connects VLPFC and posterior aspects of DLPFC in one hemisphere with homotopic and heterotopic regions in the other hemisphere. While the homotopic fibers connect the same regions on each side, the heterotopic connections of this pathway specifically link VLPFC with the contralateral supplemental motor area (SMA) and pre-SMA and DLPFC.

Our observations suggest that individual differences in neurotransmitter level in the left VLPFC, especially Glx, is associated with connectivity of regions of the right hemisphere that are connected to left VLPFC via the ventro-lateral callosal pathway. First, those individuals who had higher neurotransmitter levels in the left VLPFC (Glx and average; Fig. 6A and D) exhibited reduced connectivity between the somatomotor network (portions of which include the SMA and pre-SMA) and right DLPFC. These regions, SMA and DLPFC, are connected heterotopically to the left VLPFC via ventro-lateral callosal fibers. Second, individuals who had

Table 6 Association between neurotransmitters and temporal correlations of intrinsic networks

	SM-d	VAN-a	LMB-o	FPN-d	DMN-p	DMN-1	DMN-2
VSL-1	V_Glx-specific		D_AVG				
SM-d							V_Glx
SM-v				V_AVG			
VAN-p		V_Glx/GABA+					
LMB-o					D_GLx/GABA+, D_GABA++, D_Glx	V_Glx/GABA+	V_Glx/GABA+
FPN-v						V_Glx-specific	

Background color of a cell indicates whether the baseline correlation of the two networks is positive (orange) or negative (blue) respectively. The direction of the effect of neurotransmitter is noted by the color of the neurotransmitter label (positive: red; negative: blue)

AVG averaged level of Glx and GABA+ in that MRS voxel, *"D" and "V"* in the first column indicate the DLPFC and VLPFC MRS voxels respectively, *"Glx/GABA+"* means the ratio of Glx over GABA+. For example, the red notation of V_Glx-specific in the orange cell between VSL-1 and SM-d means that these two networks show a positive correlation at baseline and this effect is increased with increasing Glx-specific levels in the VLPFC voxel. Only those effects reaching significance at $p < 0.005$ are included in the table

higher levels of Glx in the left VLPFC exhibited reduced connectivity between the left DLPFC seed region and portions of the right DLPFC (Fig. 5A1). Here, Glx in left VLPFC could have influenced activity in right DLPFC via heterotopic ventro-lateral connections, which in turn might influence the intrinsic connectivity between contralateral DLPFC regions supported by the homotopic connections of the ventro-lateral pathway.

Other results suggest that homotopic fibers of the ventro-lateral pathway may also be involved in neurotransmitter-connectivity associations we observed. Specifically, individuals with a general overall higher level of excitatory neurotransmitter (Glx/GABA+) in left DLPFC exhibited reduced connectivity between right DLPFC and ventral portions of the fronto-parietal network (FPN-v; Fig. 6C). This effect, in which neurotransmitter level of left DLPFC is associated with connectivity of the right DLPFC, might be mediated via the homotopic ventro-lateral fibers. In addition, the neurotransmitter ratio (Glx/GABA+) in left DLPFC may also be linked to the activity of FPN-v, which significantly involves VLPFC, via heterotopic ventro-lateral fibers.

An emerging trend in these results seems to be that individuals who have higher levels of Glx in left LPFC show reduced connectivity with right hemisphere prefrontal regions to which the left LPFC is connected via the ventro-lateral callosal pathway. However, individuals with higher levels of prefrontal Glx also showed enhanced connectivity of prefrontal regions to non-prefrontal regions. For example, individuals with a higher average level of Glx and GABA + in VLPFC exhibit enhanced connectivity between left DLPFC and a site in middle temporal gyrus belonging to the dorsal frontoparietal network (FPN-d; Fig. 5A2). Besides the ventro-lateral pathway, this association may involve white matter tracts connecting prefrontal and temporal regions, likely the arcuate fasciculus. Coincidently, De Benedictis et al. (2016) reported that the ventro-lateral and arcuate fasciculus streamlines "concomitantly terminate" in the posterior part of LPFC, a fact making the involvement of arcuate fasciculus in our associations highly possible.

Therefore, at this point of time the effect of the relationship between neurotransmitters and connectivity isn't really clear. In fact, glutamatergic callosal projections of the LPFC can exert both monosynaptic excitatory and polysynaptic inhibitory effects on target neurons in the other hemisphere (Carr and Sesack 1998). Furthermore, at the theoretical level, there is a debate on whether the primary function of CC is inhibitory or excitatory (Bloom and Hynd 2005; van der Knaap and van der Ham 2011). Yet other researchers proposed that the role of CC may depend on specific task contexts, e.g., it may enhance inter-hemispheric coordination in attentional demanding situations (Banich 1998; Schulte and Müller-Oehring 2010). Considered within the context of ongoing debate, it is not clear whether the effect of higher levels of Glx in a given brain region is to increase or decrease activity in callosal-connected regions.

Left LPFC neurotransmitters are associated with connectivity of non-LPFC regions/networks

Associations within this category were obtained mostly from network-wise analyses. Once again, in most of these cases, the regions involved appear to be connected by white matter tracts. The spatial composition analysis revealed that a greater ratio of Glx to GABA in left DLFPC was related to increased connectivity between FPN-p and the right putamen (Fig. 6B). Like those associations discussed above, this effect was interhemispheric in nature, as the neurotransmitter ratio in the left DLPFC is related to connectivity involving the right putamen. Once again, regions involved in this association are directly connected by a major white matter fiber

tract. One of the three major callosal pathways originating in the LPFC as reported by De Benedictis et al. (2016) is the ventro-striatal pathway. This pathway directly connects DLPFC with the contralateral putamen and caudate nucleus. Although the location of PFN-p is remote from LPFC, it is part of the larger frontoparietal network, and accordingly its activity is highly correlated with the dorsal part of FPN (FPN-d; Fig. 4), which primarily involves DLPFC. Presumably, these three regions (left DLPFC, right putamen and FPN-d) are interrelated via polysynaptic connections, leading to the observed association pattern.

Finally, a multitude of associations was revealed regarding how individual differences in neurotransmitter level in DLPFC are associated with the temporal relationship among networks. Among them, the relationships between Glx-to-GABA+ ratio and connectivity between the orbital-frontal part of the limbic network (LMB-o) and multiple subdivision of the default mode network were observed. While these associations offer interesting information on neurochemical mechanisms that may influence network-wise communications, these effects did not pass the more stringent FWER correction and hence appear to be less reliable than the results obtained with the other two analytical approaches. As such, future replications would be needed to determine their robustness.

Relationships to prior studies

When comparing our findings with previous studies examining levels of GABA+ and Glx with regional brain connectivity, several differences are notable. First, in previous studies, usually only the connectivity of the region where neurotransmitters were measured was reported to be related to neurotransmitter concentrations (Horn et al. 2010; Lianne et al. 2012; Duncan et al. 2013; Kapogiannis et al. 2013; Stagg et al. 2014; Delli Pizzi et al. 2017; Shukla et al. 2019). In contrast, we observed multiple cases where local neurotransmitters influencing connectivity of regions outside the specific neurotransmitter-measuring region, although many are still within the larger LPFC. We speculate that the top-down regulatory role of LPFC may have allowed it to have broader impact of neural activity across the brain. In addition, most previous study limited their analyses to selected regions of interest. In contrast, we employed whole-brain analyses, which although are computationally expensive, allow us to detect any possible associations.

Second, many of the highly significant associations we observed have a clear relationship to interhemispheric connectivity, where individual differences in neurotransmitter levels of left LPFC are associated with connectivity involving a right-sided region. In at least some cases, the right-sided region is neither homotopic to the MRS voxel involved, nor homotopic to the region with which it is functionally connected. To our knowledge, this pattern has never been reported previously. Whether it is specific to LPFC neurotransmitters is not clear. But as discussed above, there appears to be an anatomical basis for such relationships. Moreover, although the great majority of callosal projections in LPFC are homotopic, as they are elsewhere in the brain, it has been suggested that heterotopic callosal projections in LPFC are richer in topographic origin than lower-level regions, e.g., the occipital cortex (Barbas et al. 2005; Jarbo et al. 2012).

Third, in addition to the specific levels each of Glx and GABA+, the average of Glx and GABA+, meant to index their common chemical pathway, was found to be related to multiple aspects of intrinsic connectivity. The impact of this overall neurotransmitter level also is usually not reported in previous studies. Yet we found robust relationships between these average values and network organization, and as such this variable may be important to examine in future studies.

Implications for clinical syndromes

The relevance of these neurotransmitter-connectivity associations to behavior or psychopathology is not yet clear. However, our work suggests a couple of potential directions. First, symptoms of schizophrenia have been linked to reduced interhemispheric functional connectivity between other PFC regions (e.g., VLPFC and medial PFC; Bleich-Cohen et al. 2012; Mwansisya et al. 2013; Chang et al. 2019). Moreover, glutamatergic theories of schizophrenia suggest that symptoms of schizophrenia may partially due to reduced NMDA (*N*-methyl-d-aspartic acid) receptor activity, which is a type of glutamatergic receptor activity, specifically in the PFC (Carlsson et al. 2001; Donald and Joseph 2001; Moghaddam and Javitt 2012). Our results suggested a link between interhemispheric intrinsic connectivity of LPFC and Glx concentration in LPFC. Taken together, it seems a promising research direction for schizophrenia studies to combine MRS and fMRI techniques to focus on glutamatergic activity in reference to the connectivity of the LPFC.

Second, our results revealed an interrelationship between individual differences in Glx levels in LPFC, interhemispheric corticocortical intrinsic connectivity and interhemispheric cortico-striatal intrinsic connectivity. Interestingly all of these brain features have been linked to substance abuse. Disturbance in cortico-striatal glutamate transmission has long been implicated in addiction-related behaviors (Kenny and Markou 2004; Kalivas et al. 2009). Moreover, individuals with substance use disorders showed reduced functional connectivity between the PFC regions in opposite hemispheres (Kelly et al. 2011; Qiu et al. 2017; Lin et al. 2018; Yu et al. 2018). We speculate that perhaps substance use disorder might also weaken connectivity

involving the PFC and striatum in opposite hemispheres, as one of our results showed that individuals with higher Glx-to-GABA+ ratio in DLPFC have enhanced 'FPN-d'-putamen inter-hemispheric connectivity (Fig. 6B). This finding might motivate investigating whether those individuals with higher relative ratios of prefrontal cortical excitation to hemispheres with stronger cortico-striatal connection might be less vulnerable to substance abuse.

Limitations

In considering our results, there are several limitations that should be considered. First, we only obtained data on adult females, given the larger study within which this investigation was embedded. Hence, the degree to which our findings generalize across genders remains to be seen. Second, due to time limitations, as MRS acquisition time is approximately one-half hour per voxel, it was not possible to obtain spectroscopy measures from voxels in the right hemisphere to examine laterality effects, nor to obtain spectroscopy measures from a non-frontal voxel (e.g., visual cortex), with which to contrast our findings. Nonetheless, each MRS voxel can be viewed as a control voxel for the other, especially considering that quite distinct patterns were observed for each.

Third, the MRS voxels were defined in the participant's native structural space according to individual's anatomical structure. This procedure allows high precision in the positioning of the voxels (in DLPFC and VLPFC). However, it leads to a variation in voxel size across participants. Nonetheless, this should not be an issue for a number of reasons. One reason is that the concentration of a given neurotransmitter is computed with regards to a standard, in this case, water within the same voxel. In that regard, all neurotransmitter values are referenced to a compound drawn from a voxel of the same size. Another reason is that in our analyses the concentration of neurotransmitter is adjusted for grey matter proportion in the voxel as these neurotransmitters are mainly expressed in grey matter, which takes into account any variation in the proportion of grey matter across voxels.

Fourth, our analyses incorporate data from multiple brain imaging modalities thus require co-registration of data from different imaging spaces. When multiple times of co-registration were applied, errors may accumulate. The seed-based analysis may be at higher risk for such kind of error. The MRS voxels defined in the subject's native structural space were first normalized to the MNI space where the seed regions were determined. Then seed regions were projected to subject' native functional space to extract their time series. In contrast, other methods involve less co-registrations and may suffer less from such error. Therefore, we suggest to comprehensively consider results from different analyses as these they tend to complement one another.

Finally, our results cannot address issues of causality. For example, currently there is no scientific data on the pattern of individual differences levels in neurotransmitter levels of Glx and GABA+ across the brain. For example, it may be that some of our results reflect a strong baseline correlation between neurotransmitter levels in two regions which are associated with patterns of connectivity. For example, it may be that individual differences in average levels of the neurotransmitter in VLFPC and temporal regions are negatively correlated, leading to an observed negative correlation between levels of activity between these two regions. On the other hand, it may be that level of neurotransmitters in VLPFC modulates connectivity of temporal regions, so as to modulate processing depending on task demands. And still another possibility is that activity in temporal regions sends a feedback signal to prefrontal regions. Disentangling these possibilities will require future research.

Conclusions

In conclusion, we observed robust associations between individual differences in levels of Glx and GABA+ in left LPFC with multiple aspects of intrinsic connectivity of regions or networks both within and beyond the LPFC. These associations often manifested with an obvious interhemispheric feature in which individual differences in levels of left LPFC neurotransmitters were associated with connectivity of a contralateral (i.e., right hemisphere) cortical or subcortical (i.e., putamen) area. Moreover, specific neurotransmitter-connectivity associations correspond to known white matter pathways, therefore offering a plausible neuroanatomical bases for these relationships. Our data do not support a simple rule for such neurotransmitter-connectivity associations (e.g., increased connectivity with higher levels of glutamate, decreased connectivity with higher levels of GABA) as was suggested by Duncan et al. (2014). Instead, considering the intricate neural circuits of LPFC, we suggest specific relationships between neurotransmitters and connectivity should be considered on a case-by-case basis with reference to known aspects of neuroanatomy.

Acknowledgements The research reported in this study was supported by NIMH Grant R01 105501 to MTB and BLK.

Compliance with ethical standards

Conflict of interest The authors declare no competing financial interests.

References

Antonenko D, Schubert F, Bohm F, Ittermann B, Aydin S, Hayek D, Grittner U, Flöel A (2017) tDCS-induced modulation of GABA

levels and resting-state functional connectivity in older adults. J Neurosci 37:4065–4073
Attwell D, Laughlin SB (2001) An energy budget for signaling in the grey matter of the brain. J Cereb Blood Flow Metab 21:1133–1145
Badre D, Wagner AD (2007) Left ventrolateral prefrontal cortex and the cognitive control of memory. Neuropsychologia 45:2883–2901
Bak LK, Schousboe A, Waagepetersen HS (2006) The glutamate/GABA-glutamine cycle: aspects of transport, neurotransmitter homeostasis and ammonia transfer. J Neurochem 98:641–653
Banich MT (1998) The missing link: the role of interhemispheric interaction in attentional processing. Brain Cogn 36:128–157
Banich MT (2009) Executive function: the search for an integrated account. Curr Dir Psychol Sci 18:89–94
Barbas H, Hilgetag CC, Saha S, Dermon CR, Suski JL (2005) Parallel organization of contralateral and ipsilateral prefrontal cortical projections in the rhesus monkey. BMC Neurosci 6:32
De Benedictis A, Petit L, Descoteaux M, Marras CE, Barbareschi M, Corsini F, Dallabona M, Chioffi F, Sarubbo S (2016) New insights in the homotopic and heterotopic connectivity of the frontal portion of the human corpus callosum revealed by microdissection and diffusion tractography. Hum Brain Mapp 37:4718–4735
Bleich-Cohen M, Sharon H, Weizman R, Poyurovsky M, Faragian S, Hendler T (2012) Diminished language lateralization in schizophrenia corresponds to impaired inter-hemispheric functional connectivity. Schizophr Res 134:131–136
Bloom JS, Hynd GW (2005) The role of the corpus callosum in interhemispheric transfer of information: excitation or inhibition? Neuropsychol Rev 15:59–71
Bullmore ET, Suckling J, Overmeyer S, Rabe-Hesketh S, Taylor E, Brammer MJ (1999) Global, voxel, and cluster tests, by theory and permutation, for a difference between two groups of structural MR images of the brain. IEEE Trans Med Imaging 18:32–42
Buzsáki G, Kaila K, Raichle M (2007) Inhibition and Brain Work. Neuron 56:771–783
Carlsson A, Waters N, Holm-Waters S, Tedroff J, Nilsson M, Carlsson ML (2001) Interactions between monoamines, glutamate, and GABA in schizophrenia: new evidence. Annu Rev Pharmacol Toxicol 41:237–260
Carr DB, Sesack SR (1998) Callosal terminals in the rat prefrontal cortex: synaptic targets and association with GABA-immunoreactive structures. Synapse 29:193–205
Chang X, Collin G, Mandl RCW, Cahn W, Kahn RS (2019) Interhemispheric connectivity and hemispheric specialization in schizophrenia patients and their unaffected siblings. NeuroImage Clin 21:101656
Cole Michael W, Bassett Danielle S, Power Jonathan D, Braver Todd S, Petersen Steven E (2014) Intrinsic and task-evoked network architectures of the human brain. Neuron 83:238–251
Conti F, Manzoni T (1994) The neurotransmitters and postsynaptic actions of callosally projecting neurons. Behav Brain Res 64:37–53
Deco G, Jirsa VK, McIntosh AR (2010) Emerging concepts for the dynamical organization of resting-state activity in the brain. Nat Rev Neurosci 12:43
Delli Pizzi S, Chiacchiaretta P, Mantini D, Bubbico G, Edden RA, Onofrj M, Ferretti A, Bonanni L (2017) GABA content within medial prefrontal cortex predicts the variability of fronto-limbic effective connectivity. Brain Struct Funct 222:3217–3229
Donahue MJ, Near J, Blicher JU, Jezzard P (2010) Baseline GABA concentration and fMRI response. NeuroImage 53:392–398
Donald CG, Joseph TC (2001) The emerging role of glutamate in the pathophysiology and treatment of schizophrenia. Am J Psychiatry 158:1367–1377
Douglas RJ, Martin KAC (2004) Neuronal circuits of the neocortex. Annu Rev Neurosci 27:419–451
Duncan NW, Wiebking C, Tiret B, Marjańska M, Hayes DJ, Lyttleton O, Doyon J, Northoff G (2013) Glutamate concentration in the medial prefrontal cortex predicts resting-state cortical-subcortical functional connectivity in humans. PLoS ONE 8:e60312
Duncan NW, Wiebking C, Northoff G (2014) Associations of regional GABA and glutamate with intrinsic and extrinsic neural activity in humans—a review of multimodal imaging studies. Neurosci Biobehav Rev 47:36–52
Edden RA, Puts NA, Harris AD, Barker PB, Evans CJ (2014) Gannet: a batch-processing tool for the quantitative analysis of gamma-aminobutyric acid–edited MR spectroscopy spectra. J Magn Reson Imaging 40:1445–1452
Eklund A, Nichols TE, Knutsson H (2016) Cluster failure: Why fMRI inferences for spatial extent have inflated false-positive rates. Proc Natl Acad Sci 113:7900–7905
Fadiga L, Craighero L, D'Ausilio A (2009) Broca's area in language, action, and music. Ann N Y Acad Sci 1169:448–458
Fame RM, MacDonald JL, Macklis JD (2011) Development, specification, and diversity of callosal projection neurons. Trends Neurosci 34:41–50
Fox MD, Raichle ME (2007) Spontaneous fluctuations in brain activity observed with functional magnetic resonance imaging. Nat Rev Neurosci 8:700
Grodzinsky Y, Santi A (2008) The battle for Broca's region. Trends Cogn Sci 12:474–480
Guo CC, Kurth F, Zhou J, Mayer EA, Eickhoff SB, Kramer JH, Seeley WW (2012) One-year test–retest reliability of intrinsic connectivity network fMRI in older adults. NeuroImage 61:1471–1483
Hankin BL, Young JF, Abela JR, Smolen A, Jenness JL, Gulley LD, Technow JR, Gottlieb AB, Cohen JR, Oppenheimer CW (2015) Depression from childhood into late adolescence: influence of gender, development, genetic susceptibility, and peer stress. J Abnorm Psychol 124:803
Harris AD, Puts N, Edden RAE (2015) Tissue correction for GABA-edited MRS: considerations of voxel composition, tissue segmentation, and tissue relaxations. J Magn Reson Imaging 42:1431–1440
Hayasaka S, Nichols TE (2003) Validating cluster size inference: random field and permutation methods. NeuroImage 20:2343–2356
Horn D, Yu C, Steiner J, Buchmann J, Kaufmann J, Osoba A, Eckert U, Zierhut K, Schiltz K, He H, Biswal B, Bogerts B, Walter M (2010) Glutamatergic and resting-state functional connectivity correlates of severity in major depression—the role of pregenual anterior cingulate cortex and anterior insula. Front Syst Neurosci 4:33
Iacoboni M, Zaidel E (2003) The parallel brain : the cognitive neuroscience of the corpus callosum. A Bradford Book, Cambridge
Jacobson S, Trojanowski JQ (1974) The cells of origin of the corpus callosum in rat, cat and rhesus monkey. Brain Res 74:149–155
Jarbo K, Verstynen T, Schneider W (2012) In vivo quantification of global connectivity in the human corpus callosum. NeuroImage 59:1988–1996
Kalivas PW, LaLumiere RT, Knackstedt L, Shen H (2009) Glutamate transmission in addiction. Neuropharmacology 56:169–173
Kapogiannis D, Reiter DA, Willette AA, Mattson MP (2013) Posteromedial cortex glutamate and GABA predict intrinsic functional connectivity of the default mode network. NeuroImage 64:112–119
Kelly C, Zuo X-N, Gotimer K, Cox CL, Lynch L, Brock D, Imperati D, Garavan H, Rotrosen J, Castellanos FX, Milham MP (2011) Reduced interhemispheric resting state functional connectivity in cocaine addiction. Biol Psychiat 69:684–692
Kenny PJ, Markou A (2004) The ups and downs of addiction: role of metabotropic glutamate receptors. Trends Pharmacol Sci 25:265–272

van der Knaap LJ, van der Ham IJM (2011) How does the corpus callosum mediate interhemispheric transfer? A review. Behav Brain Res 223:211–221

Lianne S, Goudriaan AE, Johan M, Wim B, Veltman DJ (2012) The association between cingulate cortex glutamate concentration and delay discounting is mediated by resting state functional connectivity. Brain Behav 2:553–562

Lieberman MD, Cunningham WA (2009) Type I and type II error concerns in fMRI research: re-balancing the scale. Soc Cogn Affect Neurosci 4:423–428

Lin H-C, Wang P-W, Wu H-C, Ko C-H, Yang Y-H, Yen C-F (2018) Altered gray matter volume and disrupted functional connectivity of dorsolateral prefrontal cortex in men with heroin dependence. Psychiatry Clin Neurosci 72:435–444

Logothetis NK, Pauls J, Augath M, Trinath T, Oeltermann A (2001) Neurophysiological investigation of the basis of the fMRI signal. Nature 412:150

Magistretti PJ, Pellerin L, Rothman DL, Shulman RG (1999) Energy on demand. Science 283:496

Marrelec G, Krainik A, Duffau H, Pélégrini-Issac M, Lehéricy S, Doyon J, Benali H (2006) Partial correlation for functional brain interactivity investigation in functional MRI. Neuroimage 32:228–237

Mescher M, Merkle H, Kirsch J, Garwood M, Gruetter R (1998) Simultaneous in vivo spectral editing and water suppression. NMR Biomed 11:266–272

Miller EK, Cohen JD (2001) An integrative theory of prefrontal cortex function. Annu Rev Neurosci 24:167–202

Moghaddam B, Javitt D (2012) From Revolution to evolution: the glutamate hypothesis of schizophrenia and its implication for treatment. Neuropsychopharmacol 37:4–15

Mwansisya TE, Wang Z, Tao H, Zhang H, Hu A, Guo S, Liu Z (2013) The diminished interhemispheric connectivity correlates with negative symptoms and cognitive impairment in first-episode schizophrenia. Schizophr Res 150:144–150

Nichols TE (2012) Multiple testing corrections, nonparametric methods, and random field theory. NeuroImage 62:811–815

Nickerson LD, Smith SM, Öngür D, Beckmann CF (2017) Using dual regression to investigate network shape and amplitude in functional connectivity analyses. Front Neurosci-Switz 11:115

Petroff OAC (2002) Book review: GABA and glutamate in the human brain. The Neuroscientist 8:562–573

Provencher SW (1993) Estimation of metabolite concentrations from localized in vivo proton NMR spectra. Magn Reson Med 30:672–679

Qiu Y-w, Jiang G-h, Ma X-f, Su H-H, Lv X-f, Zhuo F-z (2017) Aberrant interhemispheric functional and structural connectivity in heroin-dependent individuals. Addict Biol 22:1057–1067

Reubi JC, Van Der Berg C, Cuénod M (1978) Glutamine as precursor for the GABA and glutamate trasmitter pools. Neurosci Lett 10:171–174

Rock C, Zurita H, Lebby S, Wilson CJ, Aj A (2017) Cortical circuits of callosal GABAergic neurons. Cereb Cortex 28:1154–1167

Roland JL, Snyder AZ, Hacker CD, Mitra A, Shimony JS, Limbrick DD, Raichle ME, Smyth MD, Leuthardt EC (2017) On the role of the corpus callosum in interhemispheric functional connectivity in humans. Proc Natl Acad Sci 114:13278–13283

Salimi-Khorshidi G, Douaud G, Beckmann CF, Glasser MF, Griffanti L, Smith SM (2014) Automatic denoising of functional MRI data: combining independent component analysis and hierarchical fusion of classifiers. NeuroImage 90:449–468

Schulte T, Müller-Oehring EM (2010) Contribution of callosal connections to the interhemispheric integration of visuomotor and cognitive processes. Neuropsychol Rev 20:174–190

Shehzad Z, Kelly AMC, Reiss PT, Gee DG, Gotimer K, Uddin LQ, Lee SH, Margulies DS, Roy AK, Biswal BB, Petkova E, Castellanos FX, Milham MP (2009) The resting brain: unconstrained yet reliable. Cereb Cortex 19:2209–2229

Shukla DK, Wijtenburg SA, Chen H, Chiappelli JJ, Kochunov P, Hong LE, Rowland LM (2019) Anterior cingulate glutamate and GABA associations on functional connectivity in schizophrenia. Schizophr Bull 45(3):647–658. https://doi.org/10.1093/schbul/sby075

Smith SM, Fox PT, Miller KL, Glahn DC, Fox PM, Mackay CE, Filippini N, Watkins KE, Toro R, Laird AR, Beckmann CF (2009) Correspondence of the brain's functional architecture during activation and rest. Proc Natl Acad Sci 106:13040–13045

Smith SM, Nichols TE, Vidaurre D, Winkler AM, Behrens TEJ, Glasser MF, Ugurbil K, Barch DM, Van Essen DC, Miller KL (2015) A positive-negative mode of population covariation links brain connectivity, demographics and behavior. Nat Neurosci 18:1565

Snyder HR, Banich MT, Munakata Y (2014) All competition is not alike: neural mechanisms for resolving underdetermined and prepotent competition. J Cognitive Neurosci 26:2608–2623

Snyder HR, Friedman NP, Hankin BL (2019) Transdiagnostic mechanisms of psychopathology in youth: executive functions, dependent stress, and rumination. Cogn Ther Res 43:834–851

Stagg CJ, Bachtiar V, Amadi U, Gudberg CA, Ilie AS, Sampaio-Baptista C, O'Shea J, Woolrich M, Smith SM, Filippini N, Near J, Johansen-Berg H (2014) Local GABA concentration is related to network-level resting functional connectivity. eLife 3:e01465

Tanji J, Hoshi E (2008) Role of the lateral prefrontal cortex in executive behavioral control. Physiol Rev 88:37–57

Winkler AM, Ridgway GR, Webster MA, Smith SM, Nichols TE (2014) Permutation inference for the general linear model. NeuroImage 92:381–397

Woo C-W, Krishnan A, Wager TD (2014) Cluster-extent based thresholding in fMRI analyses: pitfalls and recommendations. NeuroImage 91:412–419

Yarkoni T (2009) Big correlations in little studies: inflated fMRI correlations reflect low statistical power—commentary on Vul et al. (2009). Perspect Psychol Sci 4:294–298

Yeo BT, Krienen FM, Sepulcre J, Sabuncu MR, Lashkari D, Hollinshead M, Roffman JL, Smoller JW, Zollei L, Polimeni JR, Fischl B, Liu H, Buckner RL (2011) The organization of the human cerebral cortex estimated by intrinsic functional connectivity. J Neurophysiol 106:1125–1165

Yu D, Yuan K, Bi Y, Luo L, Zhai J, Liu B, Li Y, Cheng J, Guan Y, Xue T, Bu L, Su S, Ma Y, Qin W, Tian J, Lu X (2018) Altered interhemispheric resting-state functional connectivity in young male smokers. Addict Biol 23:772–780

Zhang Y, Brady M, Smith S (2001) Segmentation of brain MR images through a hidden Markov random field model and the expectation-maximization algorithm. IEEE Trans Med Imaging 20:45–57